BASIN IRRIGATION DESIGN WITH LONGITUDINAL SLOPE

César González[1], Luis Cervera[2] and David Moret-Fernández[3]

1 Ph.D. Assistant Professor, Fluid Mechanics Dpt., University of Zaragoza, Spain
2 Agricultural Engineer, Fluid Mechanics Dpt., University of Zaragoza, Spain
3 Ph.D. Agricultural Engineer, Soil and Water Dpt., EEAD, Spanish Research Council (CSIC), Spain

Corresponding author:

Dr. César González Cebollada
Postal adress: EPS Carretera de Cuarte, s/n, 22197 Huesca, Spain
Telephone number: (+34) 974239301
Fax number: (+34) 974239302
Main e-mail: cesargon@unizar.es
Secondary e-mail: bronislav999@hotmail.com

ABSTRACT

The aims of this paper are to analyze theoretically the influence of the longitudinal slope of a surface irrigation field on the uniformity of irrigation and to provide practical tools to design, analyze and manage surface irrigation systems with longitudinal slope and blocked end. An example is shown where a 20% savings in water is obtained by giving the field the optimal slope.

In 1982, Clemmens and Dedrick published a practical set of dimensionless graphs to level-basin design and analysis (with no slope). This article generalizes those graphs taking account the existence of field slope. So, Clemmens and Dedrick's graphs are a particular case of obtained results.

The analysis is based on solving one-dimensional free surface Saint-Venant equations including infiltration, applying the dimensional analysis to reduce the number of variables involved. Saint-Venant equations are solved with the finite differences method, applying the full hydrodynamic model and the zero-inertia model. Two computer programs are used: WinSRFR and POZAL (a specific software that calculates the optimal cutoff time).

The result is a set of three-dimensional graphs that show the relationships of field slope, irrigation uniformity and the rest of the involved dimensionless variables, related to infiltration parameters, Manning roughness coefficient, cutoff time, inflow rate and field length and width. The graphs could be useful in practice to determine the optimal slope of a field, the inflow rate or the length and width of a field, achieving substantial savings of water in surface irrigation.

1. INTRODUCTION AND OBJECTIVES

In surface irrigation, the main water losses are usually deep percolation (water infiltrated in the land beyond the effective range of the crop roots) and, when the end field is open, surface runoff (Walker and Skogerboe, 1987).

Surface irrigation is not uniform because there is greater opportunity time for the infiltration of water in the areas closest to the supply point. In any variant of surface irrigation (basin, border, furrow, with open or blocked end) the standard uniformity is lower than pressure irrigation uniformity (sprinkle, drip). The application efficiency (*AE*) and distribution uniformity (*DU*) of surface irrigation are smaller in surface irrigation than in pressurized irrigation, although in certain situations the values might be comparable. Studies aimed at improving the efficiency of surface irrigation are usually linked to the analysis of irrigation, its frequency, flow rate (with variable flow irrigation techniques and pulse flow), cutoff time and dimensions of the fields (length and width). The related bibliography offers practical recommendations for the design and management of surface irrigation (Walker and Skogerboe, 1987; FAO, 2002). Thus, typical values for *AE* are between 50 % and 80 %, as we can see in table 1, extracted from (De Paco, 1992) which used data from the National Resources Conservation Service (NRCS) and the International Commission on Irrigation and Drainage (ICID).

Table 1. Surface irrigation application efficiency (*AE*).

When the field end is blocked (no runoff) and minimal infiltration matches required infiltration, application efficiency (*AE*), defined as the ratio between the amounts of water irrigation in the root zone after irrigation divided by the amounts of water applied, matches the distribution uniformity (*DU*), defined here as the ratio between minimum infiltration depth and infiltrated average depth.

The growing need for saving water and modern techniques of land leveling (laser or GPS), with or without slope, justify this study of field slope effect on surface irrigation performance. As an example, Figure 1 shows how the longitudinal slope of a particular basin influences the distribution uniformity.

Figure 1. Influence of the longitudinal slope on cutoff time and distribution uniformity (*DU*).

This figure was obtained by successive simulations with WinSRFR software, developed by the Arid-Land Agricultural Research Center of the USA Department of Agriculture (Bautista *et al.*, 2009). In this analyzed case, when the field has no slope, *DU* is 79.3%, but with a slight slope of 4 per 10000, *DU* is 95.8 %. In terms of saving water, the first case needs a volume of 1266.0 m^3, and the second case needs only 1040.4 m^3 (saving 225.6 m^3 of water, or 21.68 %). This lower water consumption would not have an impact on the crop, because the saved water would be lost in deep percolation.

This lower use of water is reflected also in cutoff time, as seen in Figure 1. Cutoff time is defined as the time needed to reach the required depth across the field. Without slope, cutoff time is 211 minutes, but with the slope of 0.0004, cutoff time is 173.4 minutes. Therefore the time for irrigation is reduced by 37.6 minutes, representing 17.82 % of the initial cutoff time.

2. METHODOLOGY

Clemmens *et al.* (1981) applied the technique of dimensional analysis (Bridgman, 1922) to the hydrodynamic problem of irrigation of a level basin with blocked end, for analyzing the dependency of the distribution uniformity with other relevant parameters.

$$DU = \Psi(k,a,n,t_{co},q_{in},L) \qquad (1)$$

In expression (1), DU is the distribution uniformity (defined as the minimum infiltration depth z_n divided by the average infiltration z_g); k and a are the parameters of the function of infiltration of Kostiakov; n is the Manning coefficient; t_{co} is the cutoff time; q_{in} is the inflow rate per unit of width, defined as inflow rate q divided by field width b; and L is the field length. Kostiakov function (Kostiakov, 1932) relates the infiltration depth z with the opportunity time τ according to the expression (2).

$$z(\tau) = k \cdot \tau^{a} \qquad (2)$$

Cutoff time t_{co} is supposed to be the strictly necessary time to ensure that the entire field receives the required depth z_d, so that z_n=z_d.

With the Saint-Venant governing equations and a particular choice of reference variables, Clemmens *et al*. (1981) derive a new dimensionless system:

$$DU = f(a,q_{in}^{*},L^{*}) \qquad (3)$$

with

$$q_{in}^{*} = \frac{q_{in}}{Q} \qquad (4)$$

$$L^{*} = \frac{L}{X} \qquad (5)$$

$$Q = X \cdot z_n \cdot \tau_n^{-1} \qquad (6)$$

$$X = \tau_n^{2/3} \cdot z_n^{7/9} \cdot \left(\frac{n}{C_u}\right)^{-2/3} \qquad (7)$$

The reference variables choice and the process to establish equations (4) to (7) is clearly described in Strelkoff and Clemmens (1994). In (6) and (7), τ_n is the time needed to infiltrate a depth $z_n=z_d$, and C_u is a units coefficient that in the international system is 1.0 $m^{1/2}/s$. In expression (3), variables *DU* and *a* are dimensionless.

Clemmens and Dedrick (1982) took eight different values for *a* (0.1, 0.3 0.4, 0.5, 0.6, 0.7, 0.8 and 1.0) and for each of them drew a chart representing the functional relationship

$$DU = f(q_{in}^{*}, L^{*}) \qquad (8)$$

They used a hydrodynamic one-dimensional computer model of surface irrigation and executed a sufficient number of different scenarios, solving for Saint Venant equations (conservation of mass and conservation of momentum) with the finite difference method on the model of zero inertia.

The appearance of Clemmens and Dedrick graphs is shown in Figure 2.

Figure 2. Appearance of Clemmens and Dedrick (1982) graphs (*DU*: distribution uniformity; q_{in}^*: dimensionless unit inflow rate; L^*: dimensionless field length).

The Clemmens and Dedrick graphs serve as a basic reference used in the design of level basins with borders. With them one can determine the distribution uniformity as functions of q_{in}^* and L^*. In practice, this lets us properly determine the inflow rate, the length of the field or its width, with good distribution uniformity values.

Previous development starts from the premise that the field has no longitudinal slope. As seen above, to give the field a certain slope to improve the distribution uniformity may occasionally be useful. To study this case from the perspective of dimensional analysis, *S* slope would be a new independent variable.

$$DU = \Psi(k,a,n,t_{co},q_{in},L,S) \tag{9}$$

Application of the dimensional analysis (Strelkoff and Clemmens, 1994) leads now to:

$$DU = f(a,q_{in}^*,L^*,S^*) \tag{10}$$

The derived dimensionless slope S^* is proportional to real slope *S*. For convenience, we´ll use real slope. Expression (10) can be seen as a generalization of the analysis of Clemmens and Dedrick (1982) which considers any longitudinal field slope. In this new approach, the particular case $S = 0$ is equivalent to the development of Clemens and Dedrick (1982), and then expression (10) is equal to expression (3).

For the graphical representation of expression (3), Clemmens and Dedrick (1982) gave different values to the parameter *a*, on the basis that it is only possible to represent graphically functions that depend on two variables, either through contour lines (as Clemmens and Dedrick did) or through three-dimensional graphics.

The graphical representation of (10) is somewhat more complicated because an additional variable intervenes. This leads us to fix a set of specific values for two dimensionless numbers, not only for one as in the previous case. So, the total number of graphics would be increased by an order of magnitude.

For example, in expression (10) we might fix a specific set of values for *a* and $L*$. Thus, we achieve graphics representing the functional relationship between the distribution uniformity, the field slope and dimensionless unit flow rate.

$$DU = f(S, q^*_{in}) \tag{11}$$

These charts let us, for example, find the best slope of the field for given flow conditions or find a better flow rate for a given slope.

3. RESULTS

For the parameter *a*, similar values than Clemmens and Dedrick (1982) ones are taken, and for L^*, we can take a set of five values that cover a wide range of practical possibilities.

$$a \in \{0.4, 0.5, 0.6, 0.7\} \tag{12}$$

$$L^* \in \{0.3, 0.4, 0.6, 0.8, 1.0\} \tag{13}$$

Thus, we must configure 4 x 5 = 20 different graphs. Each graph must contain a sufficiently large number of simulations covering the entire plane formed by S and q_{in}^{*} dimensionless numbers. For dimensionless unit inflow rate, 13 values are taken and 15 values for slope.

$$q_{in}^{*} \in \{0.1, 0.2, 0.3, 0.4, 0.6, 0.8, 1.0, 2.0, 3.0, 4.0, 5.0, 8.0, 10.0\} \quad (14)$$

$$S \in \left\{ \begin{array}{l} 0, 0.0001, 0.0002, 0.0003, 0.0004, 0.0005, 0.0006, 0.0007, \\ 0.0008, 0.0009, 0.001, 0.002, 0.003, 0.005, 0.01 \end{array} \right\} \quad (15)$$

Then, 20 graphs are represented, with 13 x 15 = 195 simulation points in each of them. A simulation point implies a set of about eight irrigation simulations to find optimal cutoff time (when minimal infiltration z_n is equal to required infiltration z_d). In brief, the total number of simulations is 20 graphs x 195 simulation points x 8 irrigation simulations = 31,200 simulations.

3.1. Surface irrigation simulation software: WinSRFR and POZAL.

To run the 31,200 simulations, two programs were used: WinSRFR and POZAL. WinSRFR uses a zero-inertia model when slope field is slight and a kinematic-wave model when slope is high. POZAL is a program developed specifically for this work. It applies a full-hydrodynamic model with a McCormack scheme in finite differences method (Dholakia *et al*., 1998).

The main characteristic of the POZAL program is its capacity to calculate optimal cutoff time (cutoff time that gets minimum depth z_n in the field equal to required depth z_d), saving computing time. It applies the secant method to find the intersection between required depth and minimum depth function (depending on cutoff time). Figure 3 illustrates this idea.

Figure 3. Optimal cutoff time.

In the figure, minimum depth is throughout the field, so it will be zero until water reaches the field end (advance time). In the case shown, it occurs when cutoff time is about 26 minutes (advance time will be higher, because water advance continues after cutoff time). Then, minimum depth will usually occur at the end of the field, and will increase with time. So, an optimal cutoff time will cause a minimum depth equal to required depth (either excess or lack of water). As explained above, POZAL automatically finds this optimal cutoff time.

3.2. Analysis of graphs.

An example graph is shown with distribution uniformity (expressed as a percentage) for $a=0.5$ y $L^{*}=0.6$. Figure 4 shows contour lines projected over the plane corresponding to DU = 55 % and Figure 5 shows the same graph in three-dimensional view.

Figure 4. Distribution uniformity for *a=0.5 y L*=0.6*. Contour lines.

Figure 5. Distribution uniformity for *a=0.5 y L*=0.6*. Three-dimensional graph.

A black line in figures 4 and 5 shows the moment when cutoff ratio is 85%. This indicator is the ratio of advance at cutoff to field length, and when it is lower than 85%, there is an increasing risk that water will not reach the end of the field if actual conditions depart from the input data. Clemmens and Dedrick (1982) used this line as a design criteria too, a *limit for practical level-basin design*, as they titled their work.

Distribution uniformity in figures 4 and 5 shows a curved and decreasing peak, which asymptotically takes a value of $DU = 100\%$ when $S=0$ and $q_{in}^* \rightarrow \infty$ (it would be a hypothetical instant application of all the volume of required water, obviously without taking into account the ground erosion phenomena). Keeping $S=0$, when flow decreases, the uniformity of distribution also decreases, because opportunity times at the beginning of the field are longer resulting in a less homogeneous irrigation. This fact can be seen in the graphs of Clemmens and Dedrick (1982) too, whose values match with those seen in figures 4 and 5 for $S=0$.

For a given inflow rate, distribution uniformity initially increases as the slope increases and afterwards begins to decrease; an optimal slope exists. Fixing the slope, distribution uniformity first grows and then decreases when dimensionless unit inflow grows, so there is an optimal value for unit flow rate that maximizes the uniformity of distribution for a given slope. Peak distribution uniformity decreases to hypothetical values of $DU \rightarrow 0$ when $q_{in}^* \rightarrow 0$. The crest has less and less altitude (as the slope of the field increases, the optimal distribution uniformity which can be reached is less), to an asymptotic value of $DU \rightarrow 0$ when $S \rightarrow \infty$ (the field is a vertical wall, and water falls at the end of the field).

3.3. The set of graphs.

Figures 6 and 7 show the final graphs obtained. Figure 6 represents graphs for $a=0.4$ and $a=0.5$, and Figure 7 shows the cases where $a=0.6$ and $a=0.7$. Vertically, dimensionless length L^* increases from 0.3 to 1.0, making the peak lower and displacing it from down to up.

Figure 6. Graphs for a=0.4 and a=0.5 (*a*: Kostiakov exponent; L^*: dimensionless field length).

Figure 7. Graphs for a=0.6 and a=0.7 (*a*: Kostiakov exponent; L^*: dimensionless field length).

If we put together the twenty graphs, we can make some joint analysis about the shape and evolution of them. For example, we see how when increasing L^*, the peak is separated from the horizontal axis. In practice, this refers to higher flows are required for long fields. When L^* is equal to or greater than 0.8, *DU*=90% cannot be achieved without exceeding limit line. Furthermore, with high values of L^*, the peak becomes narrower, which implies a greater sensitivity of designs.

On the other hand, increased Kostiakov exponent (greater infiltration) also implies a separation of the peak from the horizontal axis: more water is required to irrigate the field. We also observe a rightward shift of the peak, which means that greater slopes are needed when infiltration rate is high.

4. APPLICATIONS.

These graphs allow us to design and analyze surface irrigation systems with longitudinal slope and blocked end. We can determine the best field slope, or the best length, or the best unit flow rate (and therefore, the best width of the field) or the best combination for a set of variables.

4.1 Determination of the best field slope.

If parameters k and a of the Kostiakov infiltration function (through field experiments or using tables), the Manning n coefficient (using tables based on soil and crop), opportunity time τ_n (from the required infiltration z_d and the function of infiltration), unit inflow rate q_{in} (dividing irrigation flow by the field width) and the field length L, are known we can calculate q_{in}^* and L^* from (4) and (5). Then, we choose the graph that best matches L^* and a. As we know q_{in}^*, we can observe what slope offers a better distribution uniformity.

For example, in the case shown in Figure 1: q_{in} is 0.002 m^2/s (dividing 100 l/s by 50 m); from equation (2) we have τ_n=16408 s; from (6) Q is $1.919 \cdot 10^{-3}$ m^2/s; from (7) X is 314.96 m. Then, from (5) L^* is near 0.6. We will take the graph corresponding to a=0.5 and L^*=0.6 (see Figure 8).

Figure 8. Example of determination of the best field slope.

As equation (4) gives q_{in}^*=1.04, the graph indicates that maximal distribution uniformity will occur when field slope is about 0.0004. This is the best slope for this field in these conditions, and theoretical distribution uniformity will be near 95%. Because z_n=z_d , application efficiency will be 95% too. In practice, these almost perfect values will not occur, but they will be the highest possible with the slope calculated in Figure 8. The obtained design point matches the black line in Figure 6, so cutoff time is about 85%; the designed slope can initially be considered valid.

This graph also offers information about sensitivity of the solution. This is an important issue, because in practice, real conditions are different from design inputs. Design points must be centered in the high parts of the graph peak, to avoid decreasing tendencies of distribution uniformity. In the graphs, vertical axis scale is not uniform, and user must remember this when analyzing solutions sensitivity to avoid false appearances in the evaluation of *DU* variations.

Figure 8 shows that, for this example, performance will drop below *DU*=0.95 with slight changes in slope or inflow rate. However, it also shows that *DU* of 0.9 is still attainable with q_{in}^*=1, but with slopes in the range 0.003-0.006. The design can be made even more robust by selecting a smaller q_{in}^* (~0.9) and a slope of 0.0005, which puts the design in the middle of the 0.9 *DU* contour. Another viable alternative is to select a slope of 0.0001, but this may result in exceeding the limit line. The graph also shows that under the given soil conditions, it is difficult to maintain a *DU*>0.85 with slopes greater than 0.0015.

4.2 Determination of the best field length.

If k, a, n, τ_n, q_{in} and S are known, we can calculate q_{in}^* and choose the graph with a value equal to the known a value. In these graphs, we obtain DU from q_{in}^* and S. We take L^* from the graph which offers a better value of DU and finally L is calculated from (5).

4.3 Determination of the best inflow rate.

If k, a, n, τ_n, L, S and b are known, we can calculate L^* from (5) and choose the corresponding L^* and a graph. From S value, we take the value of q_{in}^* that offers a greater UD. From (4) we calculate q_{in} and multiplying by the field width b we get the best inflow rate $q=b{\cdot}q_{in}$.

4.4 Determination of the best field width.

If k, a, n, τ_n, L, S and q are known, we proceed as in the previous paragraph, and once we obtain q_{in}, we calculate the field width with $b=q/q_{in}$.

4.5 Determination of two variables simultaneously.

With these graphs, several combinations of solutions can be studied when there are two or more decision variables (e.g., length and width, or slope and width) through the analysis of a defined set of possible solutions.

5. DISCUSSION AND CONCLUSIONS.

Firstly, it is important to note that a surface irrigation field with longitudinal slope and blocked end requires a precise handling of irrigation water, either furrows or basin/border systems. If more water than expected is applied, it will go to the end of the field, and some crops cannot tolerate excessive ponding. Moreover, in long fields, the end dikes must be high to avoid overflow risk.

The results must be considered as an approximation to reality. It is a one-dimensional analysis with constant parameters. In practice, infiltration function is not uniform along a field. Manning roughness coefficient and inflow rate can vary too. The effect of micro-topography is not considered here, but it is an important factor in distribution uniformity (Playán *et al*., 1996; Zapata and Playán, 2000).

However, graphs could be useful in real design and management of surface irrigation fields. In the above example, theoretical distribution uniformity and application efficiency were 95% with a slope of 0.0004 . Putting this case into practice, real values will be lower (perhaps 85%?). But in any case, calculated slope will get maximal values for both indicators, and practical recommendation for irrigator would be to consider giving this slope to the field when leveling this field, considering also the negative impacts of land leveling (costs, changes in soil characteristics and productivity).

In real cases, values for a and L^* probably will be different than discrete values taken in figures 6 and 7 and represented in expressions (12) and (13), so interpolation process have to be applied, taking values from two or more graphs.

Dimensionless graphs obtained are a continuation of Clemmens and Dedrick (1982) graphs, a kind of generalization, and could be useful when designing and management surface irrigations fields with longitudinal slope and blocked end.

REFERENCES

Bautista, E., Clemmens A.J., Strelkoff T.S., Schlegel J.L., 2009. Modern analysis of surface irrigation systems with WINSRFR. Agric. Water Manage. 96, 1146-1154.

Bridgman, P.W., 1922. Dimensional Analysis. Yale University Press.

Clemmens, A.J., Strelkoff, T.S., Dedrick, A.R., 1981. Development of solutions for level-basin design. J. Irrig. Drain. Div., ASCE 107 (3), 265-279.

Clemmens, A.J., Dedrick A.R., 1982. Limits for practical level-basin design. J. Irrig. Drain. Div., ASCE 108 (2), 127-141.

De Paco, J.L., 1992. Fundamentos del cálculo hidráulico en los sistemas de riego y drenaje. IRYDA, Ministerio de Agricultura, Pesca y Alimentación. Ediciones Mundi Prensa. ISBN 84-7114-423-9.

Dholakia, M., Misra R., Zaman, M.S., 1998. Simulation of border irrigation system using explicit MacCormack finite difference method. Agric. Water Manage. 36, 181-200.

FAO, 2002. Irrigation manual - planning, development, monitoring and evaluation of irrigated agriculture with farmer participation. Food and Agriculture Organization of the United Nations. Harare, Zimbabwe.

Playán, E., Faci, J.M., Serreta, A., 1996. Characterizing microtopographical effects on level-basin irrigation performance. Agric. Water Manage. 29, 129-145.

Strelkoff, T.S., Clemmens, A.J., 1994. Dimensional analysis in surface irrigation. Irrig. Sci. 15, 57-82.

Walker, W.R., Skogerboe, G.V., 1987. Surface irrigation, theory and practice. Prentice-Hall, Englewood Cliffs, N.J.

Zapata, N., Playán, E., 2000. Simulating elevation and infiltration in level-basin irrigation. J. Irrig. Drain. Div., ASCE 126 (2), 78-84.

Table 1. Surface irrigation application efficiency (*AE*).

Irrigation method	NRCS	ICID
Basin	60-80%	56-59%
Border	60-75%	47-57%
Furrow	50-70%	54-58%

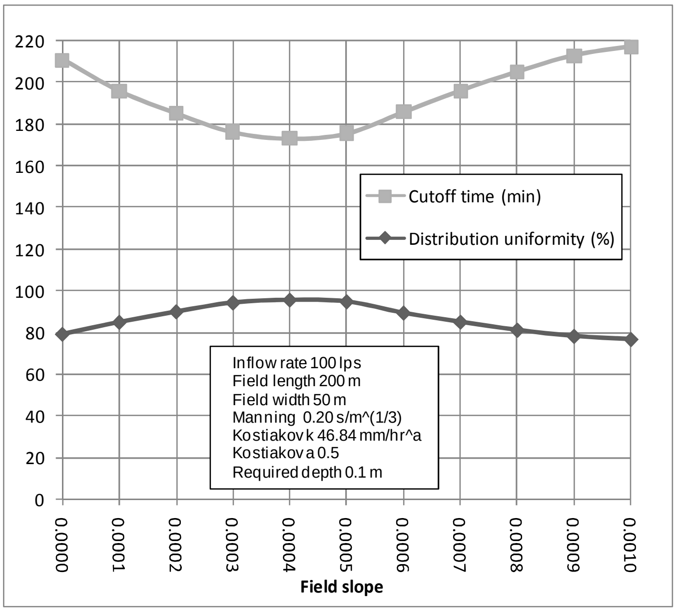

Figure 1. Influence of the longitudinal slope on cutoff time and distribution uniformity (*DU*).

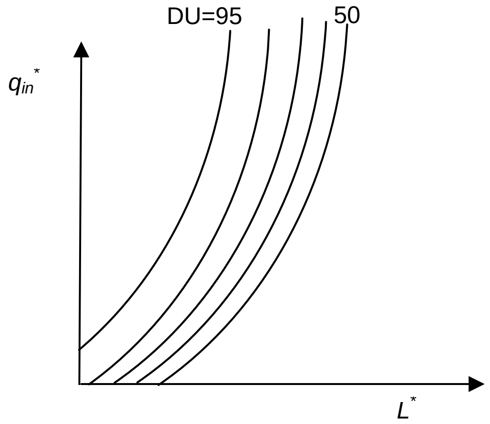

Figure 2. Appearance of Clemmens and Dedrick (1982) graphs (*DU*: distribution uniformity; q_{in}^*: dimensionless unit inflow rate; L^*: dimensionless field length).

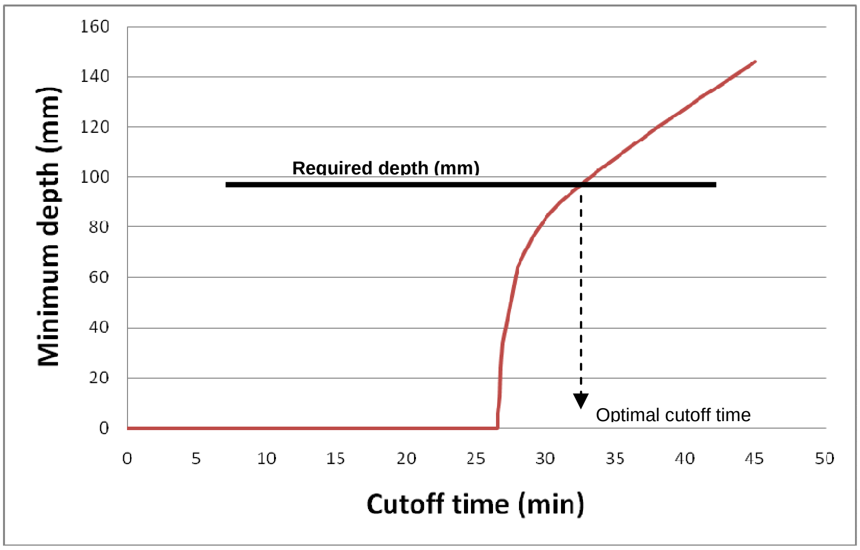

Figure 3. Optimal cutoff time.

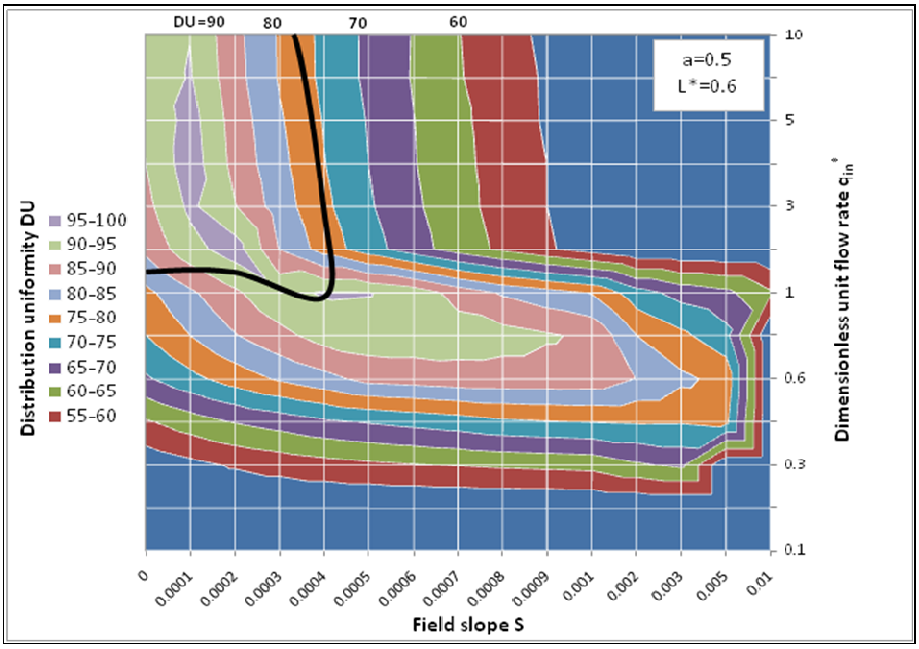

Figure 4. Distribution uniformity for *a=0.5 y L*=0.6*. Contour lines.

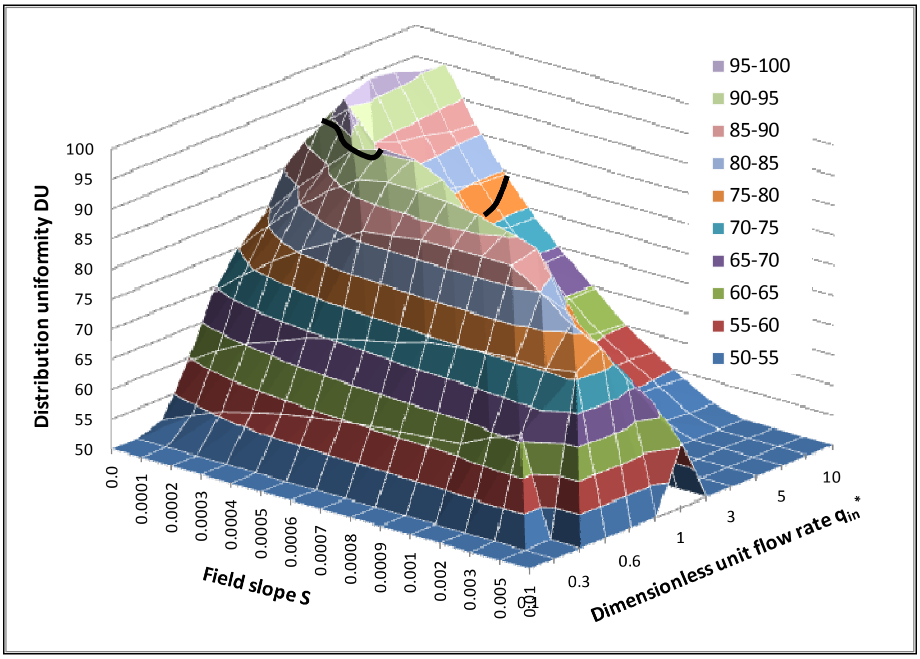

Figure 5. Distribution uniformity for *a=0.5 y L*=0.6*. Three-dimensional graph.

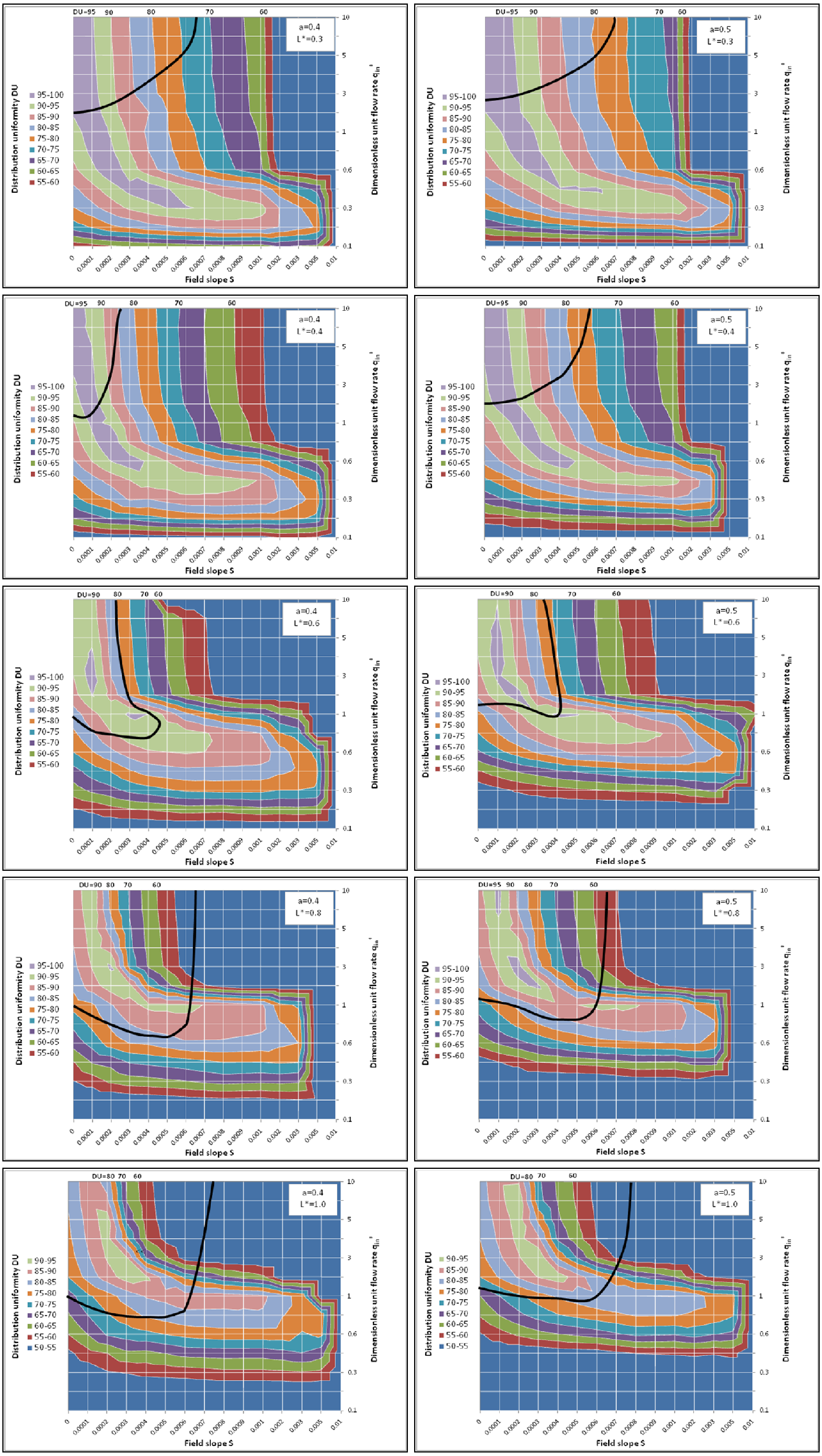

Figure 6. Graphs for a=0.4 and a=0.5 (*a*: Kostiakov exponent; L^*: dimensionless field length).

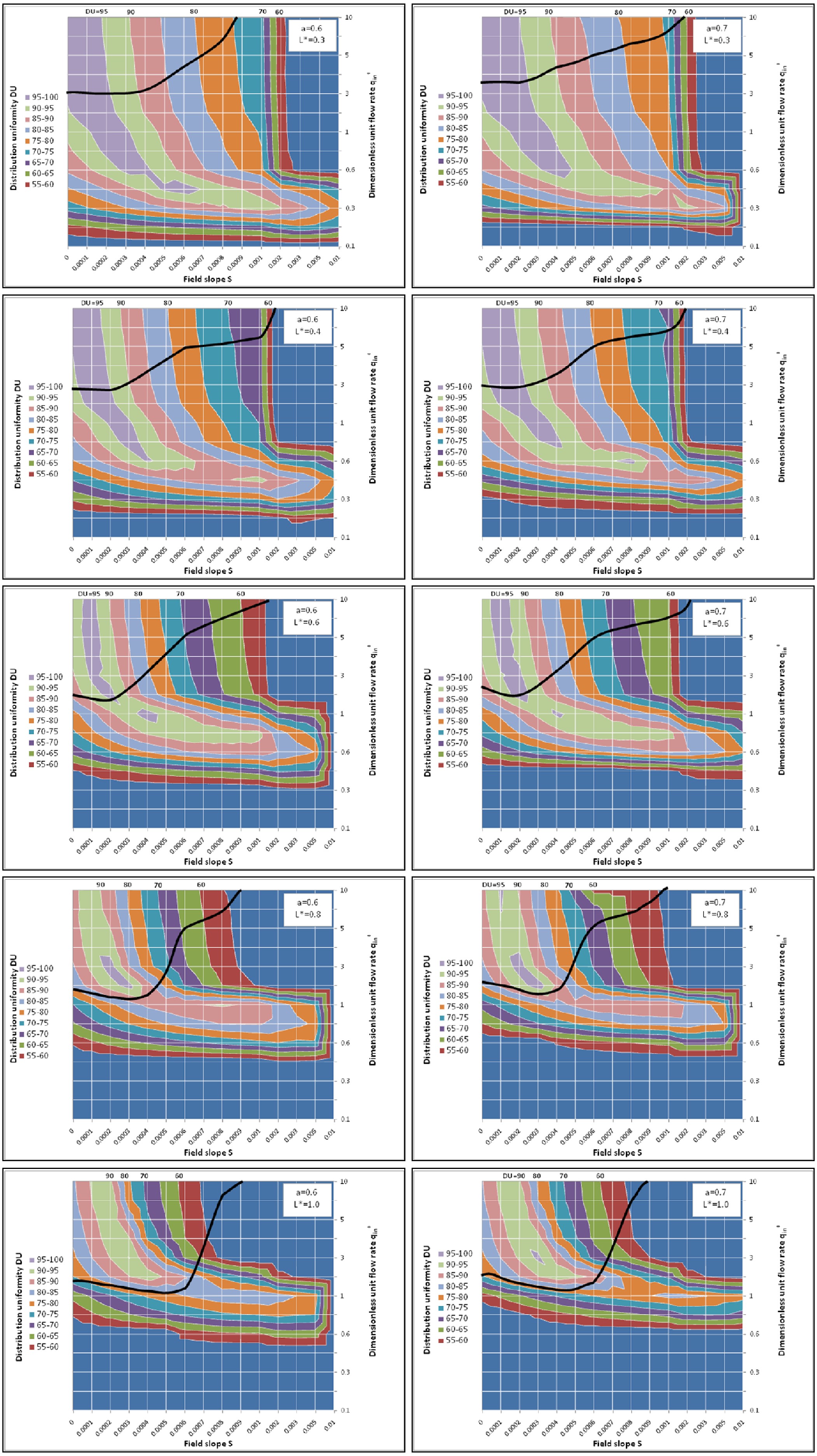

Figure 7. Graphs for a=0.6 and a=0.7 (*a*: Kostiakov exponent; L^*: dimensionless field length).

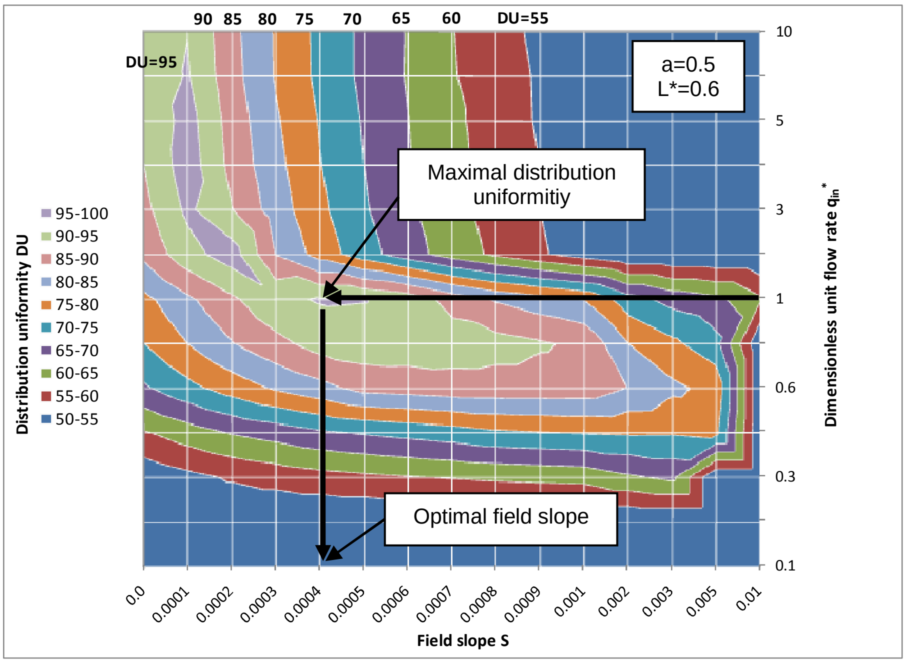

Figure 8. Example of determination of the best field slope.

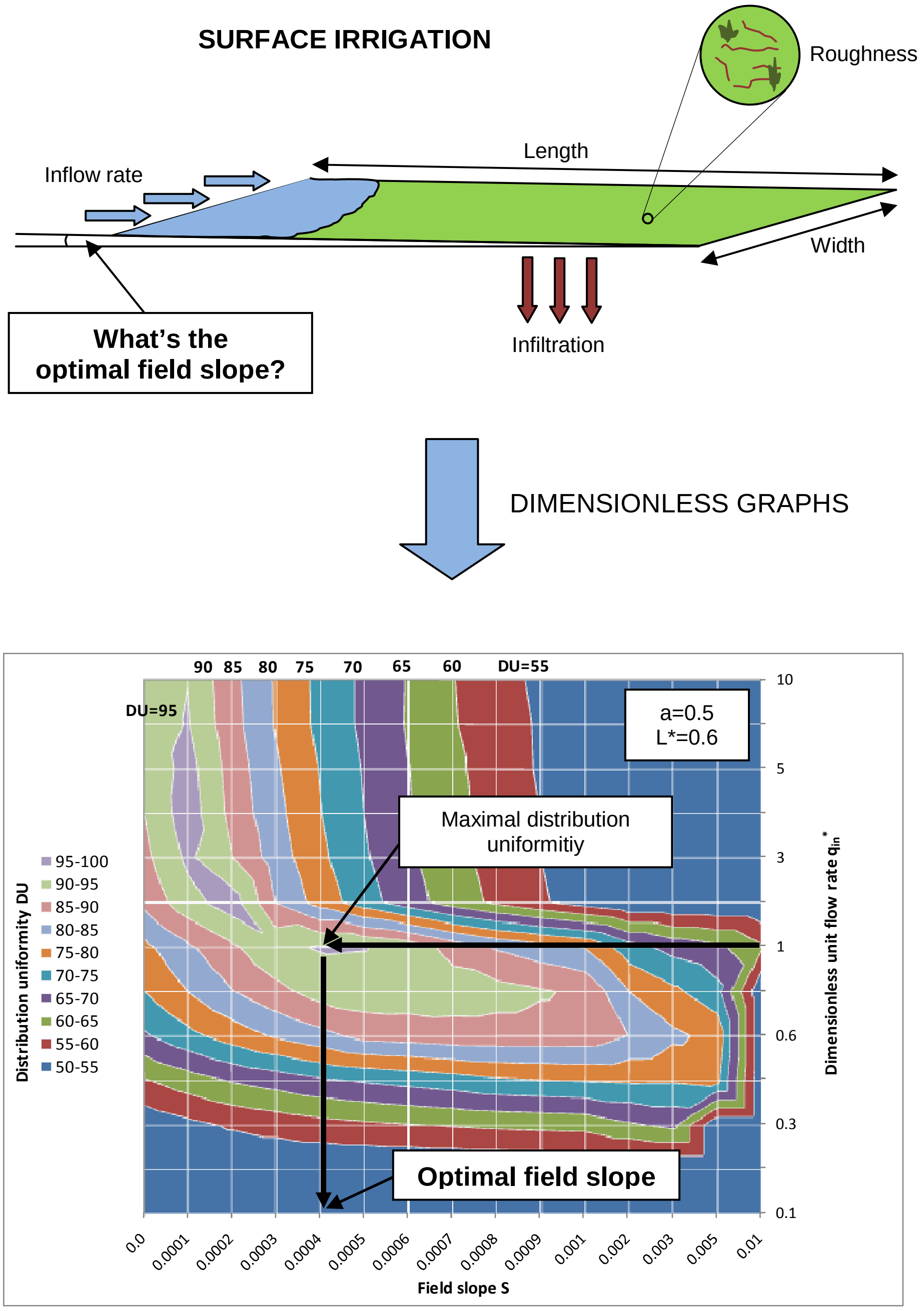
SURFACE IRRIGATION
Roughness
Length
Inflow rate
Width
Infiltration
What's the optimal field slope?
DIMENSIONLESS GRAPHS
90 85 80 75 70 65 60 DU=55
DU=95
a=0.5
L*=0.6
Maximal distribution uniformitiy
Optimal field slope
95-100
90-95
85-90
80-85
75-80
70-75
65-70
60-65
55-60
50-55
Distribution uniformity DU
Dimensionless unit flow rate q_{in}^*
10
5
3
1
0.6
0.3
0.1
0.0
0.0001
0.0002
0.0003
0.0004
0.0005
0.0006
0.0007
0.0008
0.0009
0.001
0.002
0.003
0.005
0.01
Field slope S